Heliyon 9 (2023) e20983

Contents lists available at ScienceDirect

Heliyon

journal homepage: www.cell.com/heliyon

# Computed tomography texture-based models for predicting KIT exon 11 mutation of gastrointestinal stromal tumors

Chuangen Guo [a,1], Hao Zhou [b,1], Xiao Chen [b,*], Zhan Feng [a,**]

[a] Department of Radiology, The First Affiliated Hospital, Zhejiang University School of Medicine, 79 Qingchun Road, Hangzhou, 310003, China
[b] Department of Radiology, The Affiliated Hospital of Nanjing University of Chinese Medicine, 155 hanzhong Road, Nanjing, 210029, China

ARTICLE INFO

*Keywords:*
Gastrointestinal stromal tumor
Computed tomography
Radiomics feature
KIT exon 11

ABSTRACT

*Background:* KIT exon 11 mutation in gastrointestinal stromal tumors (GISTs) is associated with treatment strategies. However, few studies have shown the role of imaging-based texture analysis in KIT exon 11 mutation in GISTs. In this study, we aimed to show the association between computed tomography (CT)-based texture features and KIT exon 11 mutation.

*Methods:* Ninety-five GISTs confirmed by surgery and identified with mutational genotype of KIT were included in this study. By amplifying the samples using over-sampling technique, a total of 183 region of interest (ROI) segments were extracted from 63 patients as training cohort. The 63 new ROI segments were extracted from the 63 patients as internal validation cohort. Thirty-two patients who underwent KIT exon 11 mutation test during 2021–2023 was selected as external validation cohort. The textural parameters were evaluated both in training cohort and validation cohort. Least absolute shrinkage and selection operator (LASSO) algorithms and logistic regression analysis were used to select the discriminant features.

*Results:* Three of textural features were obtained using LASSO analysis. Logistic regression analysis showed that patients' age, tumor location and radiomics features were significantly associated with KIT exon 11 mutation ($p < 0.05$). A nomogram was developed based on the associated factors. The area under the curve (AUC) of clinical features, radiomics features and their combination in training cohort was 0.687 (95 % CI: 0.604–0.771), 0.829 (95 % CI: 0.768–0.890) and 0.874 (95 % CI: 0.822–0.926), respectively. The AUC of radiomics features in internal validation cohort and external cohort was 0.880 (95 % CI: 0.796–0.964) and 0.827 (95%CI: 0.667–0.987), respectively.

*Conclusion:* The CT texture-based model can be used to predict KIT exon 11 mutation in GISTs.

## 1. Introduction

Gastrointestinal stromal tumors (GISTs) are the most common mesenchymal tumors of the digestive system which originate from

*Abbreviations:* AUC, area under the curve; CI, confidence interval; CT, computed tomography; GISTs, gastrointestinal stromal tumors; LASSO, Least absolute shrinkage and selection operator; OS, Overall survival; PDGFRA, platelet-derived growth factor receptor alpha; PFS, progression-free survival; OR, odds ratio; ROI, region of interest; TKIs, tyrosine kinase inhibitors.

* Corresponding author. The Affiliated Hospital of Nanjing University of Chinese Medicine, China.
** Corresponding author. The First Affiliated Hospital, Zhejiang University School of Medicine, China.
*E-mail addresses:* fsyy00597@njucm.edu.cn (X. Chen), gerxyuan@zju.edu.cn (Z. Feng).
[1] Chuangen Guo and Hao Zhou contributed equally to this work.

https://doi.org/10.1016/j.heliyon.2023.e20983
Received 21 February 2023; Received in revised form 11 October 2023; Accepted 12 October 2023
Available online 13 October 2023

the interstitial cells of the gastrointestinal pacemaker Cajal cells [1]. According to histologically heterogeneous and malignant potential of GISTs, curative surgical resection is the primary option for treatment. For patients with a high risk of recurrence, tyrosine kinase inhibitors (TKIs) treatment was recommended as an adjuvant therapy [2]. Imatinib as the first-line targeted molecular drug can recognize the "switch-off" inactive conformation of the kinase by competitively binding to the ATP-binding site [3].

Most GISTs exhibit an activated mutation in KIT protooncogene or platelet-derived growth factor receptor alpha (PDGFRA) receptor tyrosine kinase which are called KIT/PDGFRA-mutated GISTs [2]. Approximately 75%–80 % of GISTs involve KIT gene mutations and 10 % of GISTs involve PDGFRA gene mutations [2]. Unfortunately, GISTs without KIT or PDGFRA mutation account for 10%–15 % of GISTs and are historically classified as wild-type GISTs and are not sensitive to TKIs.

KIT exon 11 mutations account for more than 70 % of KIT mutations and promote tumorigenesis of GISTs [4]. GISTs with primary KIT exon 11 mutation performs the best therapy response to imatinib. Therefore, mutational profiling is important for GISTs patients who is considered for molecular targeted treatment with TKIs. In addition, KIT exon 11 mutation is also associated with prognosis [5, 6]. However, gene mutations are analyzed by genotype examinations which need surgically resected tissue samples and usually expensive. Both high cost and invasive procedure of genotype examination contribute to the reason that it cannot be a widely performed examination for most of GISTs patients [7].

Radiological assessment before treatment is convenient and necessary for GISTs patients. Computed tomography (CT) is a crucial imaging modality of choice for preoperative diagnosis. On post-contrast CT images, GISTs usually present with peculiar imaging features, such as large abdominal mass, heterogeneous enhancement and variable amount of necrosis within the tumor [8]. However, although some CT imaging predictors of malignancy have been identified and were correlated with prognosis and survival of GISTs, the analysis of CT images is influenced by the observer's subjective assessment.

Radiomics has been recognized as a promising tool in oncology which allows to quantify lesion heterogeneity, extracting additional quantitative features from radiological imaging, which cannot be evaluated by human eyes [9]. It has been widely used in tumor diagnosis, identification and prognosis predictions [10]. Previous studies have identified radiomics characters from CT images as a superior tool for risk stratification and predicting the malignancy potential of GISTs [11–13].

Recently, several studies demonstrated associations between radiomics parameters and tumor mutations in lung cancer, renal cell carcinoma, breast cancer and gastric cancer [14–17]. However, there are rare study explore the relationship between CT texture analysis and genomic phenotypes of GISTs. In this study, we aimed to explore association between CT texture parameters and KIT exon 11 mutation of GISTs and develop a predictable noninvasive model to differentiate GISTs without KIT exon 11 mutation, which were not sensitive to imatinib.

## 2. Materials and methods

### 2.1. Patients

With the ethical approval by the institutional review board of the First Affiliated Hospital of Zhejiang University School of Medicine (2017NL-137), a total of 122 patients with pathologically confirmed GISTs and gene screening were observed in our institution.

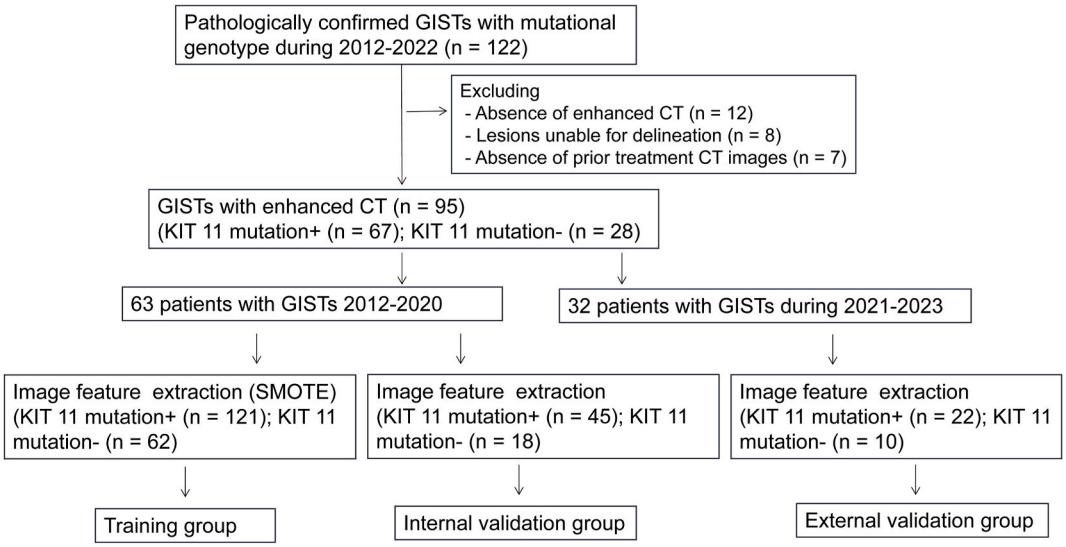


**Fig. 1.** The flowchart of study population. A total of 121 patients with pathologically confirmed GISTs and gene screening were observed in our institution. Sixty-three patients with GIST during 2012–2020 were included training and internal validation cohort. Synthetic minority oversampling technique (SMOTE) was used for training data. Thirty-one patients with GIST during 2021–2023 were included in external validation cohort.

Declaration of Helsinki was followed during the study. Informed consent was obtained from participants. The inclusion criteria of this study were as follows: (1) patients had received enhanced CT examination within 15 days of tumor resection; (2) identified with mutational genotype of KIT and PDGFRA. The exclusion criteria of this study were as follows: (1) patients had not received enhanced CT examination; (2) lesions were too small to delineate the region of interest (ROI); (3) prior treatment CT images of the patients were absent; (4) receiving any anti-tumor treatment before surgery. Finally, a total of 95 patients were included in this study (Fig. 1). Sixty-three patients who underwent KIT exon 11 mutation test during 2012–2020 was selected for training test and internal validation (population 1). Thirty-two patients who underwent KIT exon 11 mutation test during 2021–2023 was selected as external validation cohort (population 2).

### 2.2. CT scanning protocol

CT scan were performed using 64-channel CT scanner (Brilliance 64, Philips Healthcare, the Netherlands) and 128-channel iCT scanner (Brilliance 256, Philips Healthcare, the Netherlands). The scanning range was from the top of the diaphragm to the level of the lower margin of pubic symphysis with head to foot direction. The scanning parameters were as follows: Collimation of 64 × 0.625 mm, FOV of 250 mm, tube voltage of 120 kV, tube current of 250 mAs, layer thickness of 5 mm, the layer interval of 5 mm, gantry rotation time of 0.4 s, pitch of 0.891, the algorithm of Standard (B), matrix of 512 × 512, an intravenous contrast agent injection of 70–100 mL, an injection rate of 2.5–3.5 mL/s with a high-pressure syringe, routine plain scan, an arterial phase with 25–30s and a venous phase with 55–60s.

### 2.3. CT texture feature extraction and analysis

Both tumor segmentation and image radiomics feature extraction were performed using IBEX software packages based on MATLAB. ROI were delineated along the outline of the tumor on preoperative venous phase CT images of the GISTs by two experienced radiologists. Due to the limited number of cases in our study, only 2D ROI analysis was performed on axial images by referring to previous study [19]. We first sketched the axial image with the largest area of the tumor, and then segmented the upper and lower slices of the maximum slice at 2 slices intervals in turn. The necrotic areas of the tumor were avoided. All of these CT images were preprocessed using image resampling and gray value homogenization before feature extraction. Texture feature parameters including gray histogram parameters, gray co-occurrence matrix, neighbor intensity difference and gray level run length matrix were analyzed. Considering the small sample size of patients without KIT 11 mutation and the unbalanced KIT 11 mutation data of our study, we amplified the samples with a synthetic minority oversampling technique (SMOTE) in training study [18]. The SMOTE algorithm creates synthetic samples that are not merely replications. We extracted ROI segments from 3 to 5 slices of the mass without KIT 11 mutation and extracted ROI segments from 1 to 2 slices of the mass with KIT 11 mutation, respectively. Finally, a total of 183 ROI segments were extracted from these 63 patients as training group (62 ROIs for GISTs without KIT 11 mutation). For internal validation group, we extracted ROI segment from the axial image with the largest area of the tumor so that 63 ROI segments were extracted from 63 patients (18 for GISTs without KIT 11 mutation). Similarly, we extracted ROI segment from 32 ROI segments in external validation group (10 for GISTs without KIT 11 mutation).

### 2.4. Feature dimension reduction and model establishment

The LASSO (Least Absolute Shrinkage and Selection Operator) regression method was used to select and classify features of the texture data to identify the most relevant features for KIT 11 mutation. A linear combination of selected features weighted by the corresponding LASSO coefficients was used to calculate Radiomics scores (rad-scores). Then, a radiomics model was established. Besides, univariate and multivariate logistic regression were used to identify the associated clinical factors and establish a clinical model. Finally, we combined the clinical features with radiomics features to establish anther model. The parameters of sensitivity, specificity, and area under curve (AUC) were used to evaluate the predication power of these models.

### 2.5. Statistical analysis

R software (version 3.4.1) was used for feature selection, machine learning classifiers and nomogram generation, SPSS (version 26) was used for statistical analysis. Clinicopathological factors including age, sex, tumor location and tumor diameter were analyzed. Qualitative variables were described using frequency (percentage) and compared by chi-square test. Shapiro normality test was performed for continuous variables first. The data in line with normal distribution were represented by mean ± standard deviation and *t*-test was used for analysis between groups. For data with abnormal distribution, median (P50) and Mann-Whitney *U* test was adopted. Repeatability for radiomics features between two readers was evaluated by intraclass correlation coefficient (ICC). P value less than 0.05 were considered as statistical significance.

## 3. Results

### 3.1. Patient demographics and clinicopathological features of GIST

The clinical data of population is shown in Table 1. KIT 11 mutation was found in 45 of 63 patients and in 10 of 32 patients in

external validation cohort. No significant difference was found in patients' age, sex, grade and diameter between those patients with and without mutation. KIT 11 mutation was more common in stomach GISTs than extra-stomach GISTs (64.4 % vs 38.9 %, p = 0.06).

### 3.2. Imaging features selection and radiomic model establishment

63 patients were selected for segmentation and a total of 681 quantitative radiomics features with good reproducibility (ICC: 0.78–0.90) were extracted from each ROIs. Texture feature parameters including gray histogram parameters (n = 49), gray co-occurrence matrix (n = 594), neighbor intensity difference (n = 5) and gray level run length matrix (n = 33). The extracted texture parameters included gray level co-occurrence matrix (GLCM) features, gray level run length matrix (GLRLM) features, Intensity Histogram features and Neighbor Intensity Difference features. After application of LASSO logistic algorithm, 4 out of the 681 radiomics features were finally used to develop the radiomics signature for the prediction of KIT 11 mutation on the entire training dataset (Fig. 2a and b). Coefficients of the LASSO logistic regression model for calculation were visualized in Fig. 2c. Among the 4 radiomics features, X459 (GLCM feature, GrayLevelCooccurenceMatrix25-315-7InverseVariance) was excluded according to the lower coefficient weigh between radiomics features and no significant difference was found after multivariable analysis. X453 (GLCM feature, Inverse Variance, GrayLevelCooccurenceMatrix25-225-7InverseVariance) (p = 0.004), X629 (Intensity Histogram feature, IntensityHistogram-Kurtosis) (p = 0.008) and X680 (Neighbor Intensity Difference feature, NeighborIntensityDifference25-contrast) (p = 0.004) was associated with KIT 11 mutation (Table 2). Among them, the mean values of X453 and X680 were larger in GISTs with KIT 11 mutation than that without KIT 11 mutation. The mean value of X629 was lower in GISTs with KIT exon 11 mutation compared with GISTs without KIT exon 11 mutation (Fig. 3A).

Similar results were observed in internal validation group (Fig. 3B) and external validation group (Fig. 3C). Fig. 4 shows two GIST patients with and without KIT 11 mutation. Similar imaging findings and similar histological features were observed in the two cases. However, there were differences in X453 (0.52 vs 0.43), X629 (4.60 vs 5.10), and X680 (42.71 vs 36.52).

### 3.3. Diagnostic performance of the radiomics model

As shown in Table 2, clinical features (patients' age and tumor location) and radiomics features (X453, X629, X680) were identified by univariable and multivariable logistic analysis as independent predictors for GISTs with KIT 11 mutation in training cohort. Patients' age and tumor location were taken into consideration for clinical model establishment. Radiomic model was established using X453, X629 and X680. All the five variables were used to develop a combination model which was expected for further improvement of the prediction efficiency. The predictable performance of clinical features, radiomics features and their combination in predicting KIT exon 11 mutation were analyzed by ROC (Fig. 5). The area under the curves (AUC) of clinical features, radiomics features and their combination in training cohort was 0.69 (95 % CI 0.60–0.77) (sensitivity of 0.45, specificity of 0.83), 0.83 (95 % CI 0.77–0.89) (sensitivity of 0.74, specificity of 0.84) and 0.87 (95 % CI 0.82–0.93) (sensitivity of 0.89, specificity of 0.79), respectively (Fig. 5a). We also validated the predictable performance of radiomics features in an internal validation (AUC = 0.880, 95%CI 0.796–0.964, sensitivity of 0.78, specificity of 0.84) and external validation cohort (AUC = 0.83, 95%CI 0.67–0.99, sensitivity of 1.00, specificity of 0.73) (Fig. 5B and C), respectively.

### 3.4. Nomogram

Based on age, tumor location and radsore we developed a nomogram for identifying GISTs without KIT 11 mutation (Fig. 6). For a 60-year old person with extra-stomach GISTs, the point was 30 and 17, respectively. The point for a radscore of 0.5 was 50. The total point for this person was 97. The risk of absence of KIT 11 mutation was 0.55. Calibration curve also showed that the nomogram had good performance.

**Table 1**
Clinicopathological features of GIST.

| | Population 1 | | | Population 2 | | |
|---|---|---|---|---|---|---|
| | KIT 11 Mutation + (n = 45) | KIT 11 Mutation – (n = 18) | *P* | KIT 11 Mutation + (n = 22) | KIT 11 Mutation – (n = 10) | *P* |
| Age (year) | 58.80 ± 9.83 | 63.33 ± 11.63 | 0.12 | 64.09 ± 14.15 | 61.20 ± 10.60 | 0.57 |
| Sex | | | 0.33 | | | 0.45 |
| Male | 24 | 12 | | 12 | 4 | |
| Female | 21 | 6 | | 10 | 6 | |
| Location | | | 0.06 | | | 0.13 |
| Stomach | 29 | 7 | | 14 | 7 | |
| Extra-Stomach* | 16 | 11 | | 8 | 3 | |
| NIH Risk Category | | | 0.55 | | | 0.41 |
| Low * | 15 | 6 | | 7 | 2 | |
| Intermediate -High | 30 | 12 | | 15 | 8 | |
| Diameter (cm) | 5.99 ± 2.98 | 6.41 ± 3.46 | 0.64 | 7.40 ± 4.91 | 6.40 ± 2.97 | 0.56 |

Extra-Stomach*: including GISTs originate from small bowel, colorectum and mesentery.
Low*: including GISTs with very-low-risk and low-risk.

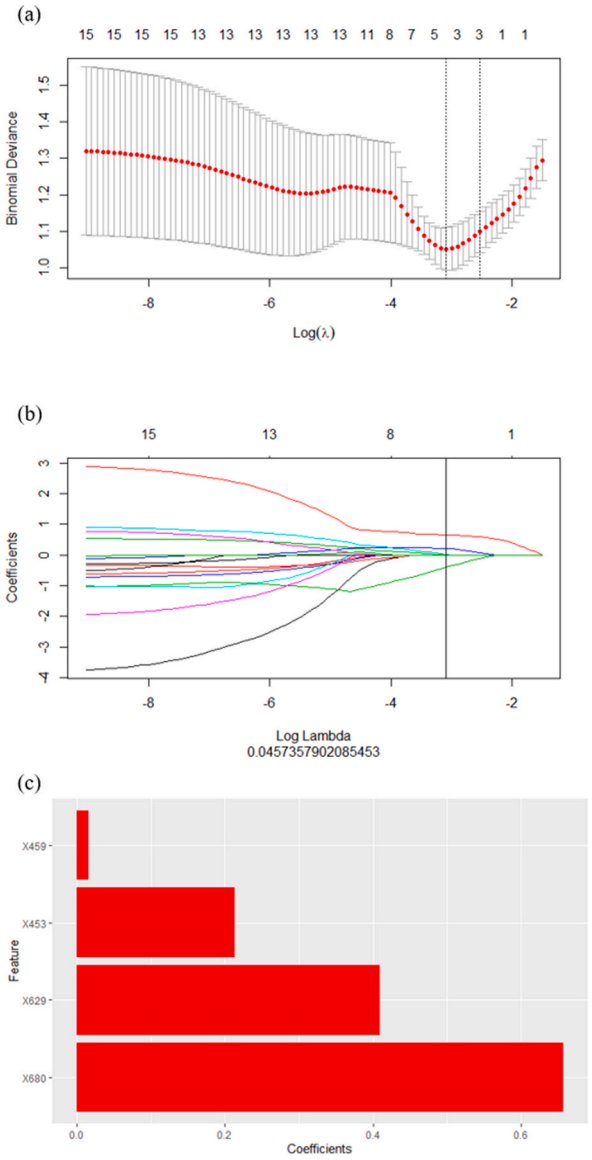


**Fig. 2.** Least absolute shrinkage and selection operator (LASSO) regression to extract the radiomics features. A: The selection of tuning parameter (λ) used 10-fold cross-validation via minimum criteria. The curve was plotted versus log (λ). B: LASSO coefficient profiles of the radiomics features. C: Four radiomics features were obtained.

**Table 2**
The associated factors with KIT 11 mutation.

| Variable | Training cohort | | | |
|---|---|---|---|---|
| | Univariable | P | Multivariable | P |
| Age (years) | 1.05 (1.02–1.08) | 0.003 | 1.06 (1.02–1.10) | 0.002 |
| Location (Stomach vs extra-Stomach) | 2.67 (1.42–5.02) | 0.002 | 3.11 (1.40–6.93) | 0.006 |
| X453 | 6.30 (2.81–14.15) | < 0.001 | 3.76 (1.54–9.17) | 0.004 |
| X629 | 0.59 (0.45–0.77) | < 0.001 | 0.68 (0.51–0.91) | 0.008 |
| X680 | 1.05 (1.03–1.07) | < 0.001 | 1.03 (1.01–1.05) | 0.004 |

X453: GLCM feature, Inverse Variance, GrayLevelCooccurenceMatrix25-225-7InverseVariance); X629: Intensity Histogram feature, IntensityHistogram-Kurtosis); X680: Neighbor Intensity Difference feature, NeighborIntensityDifference25-contrast.

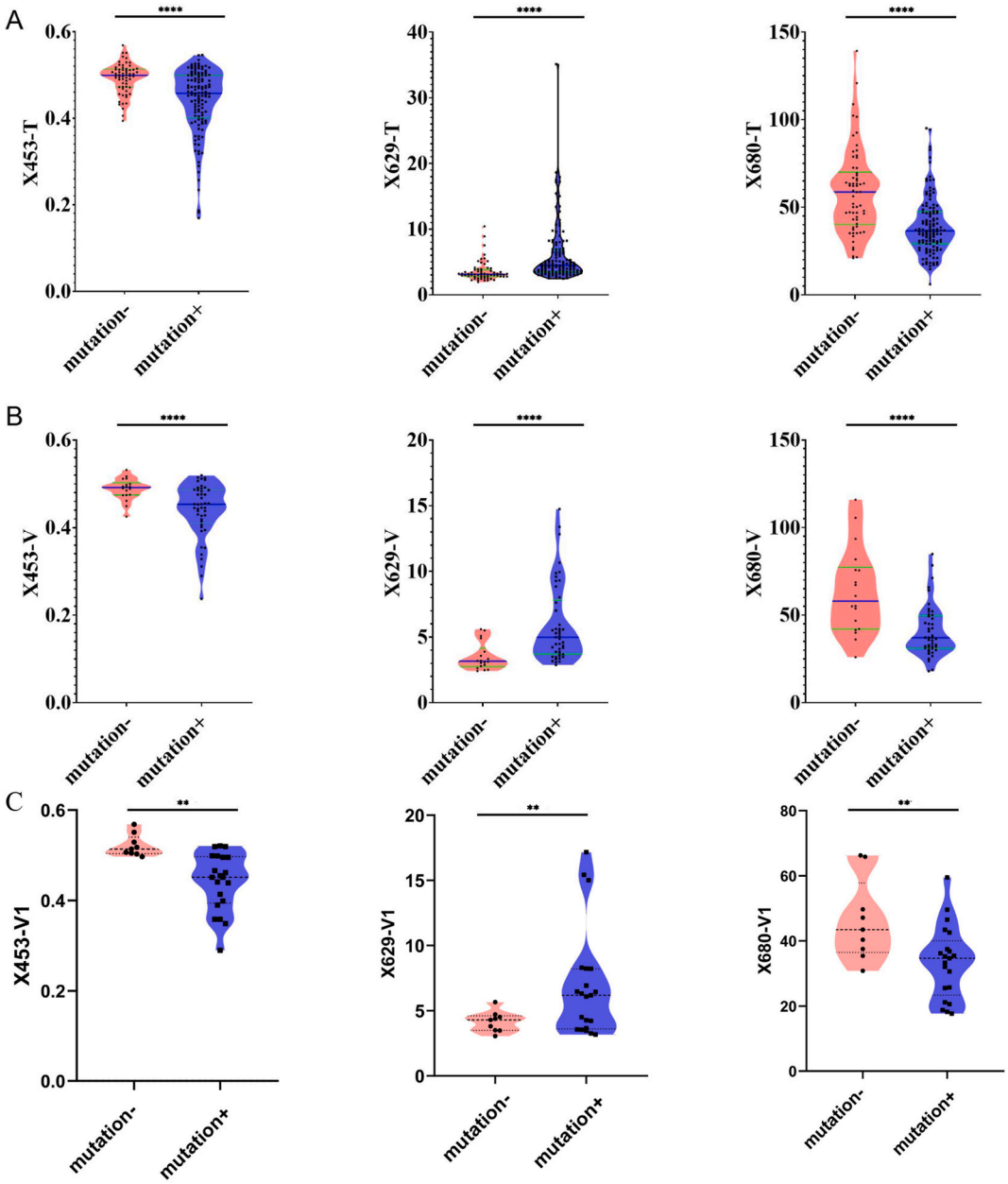


**Fig. 3.** The differences in radiomics features between tumors with and without KIT Exon 11 mutation in training (A), internal validation (B) and external validation (C) groups. Significant differences were found in X453 (GLCM feature, Inverse Variance, GrayLevelCooccurenceMatrix25-225-7InverseVariance), X629 (Intensity Histogram feature, IntensityHistogram-Kurtosis) and X680 (Neighbor Intensity Difference feature, NeighborIntensityDifference25-contrast) between tumors with and without KIT mutation. ****, $p < 0.001$; **, $p < 0.05$.

## 4. Discussion

GISTs were mesenchymal neoplasms with variable malignant potential and responded poorly to either radiotherapy or chemotherapy. Although most GISTs were localized and preferred complete surgical excision, the emergency of TKIs had modified the treatment of GISTs and was able to prolong overall survival of GISTs patients [7]. GISTs with specific gene mutation were sensitive to treatment of TKIs [20]. Studies have showed that GISTs with primary KIT exon 11 mutation were well respond to imatinib, a small-molecule TKIs [3,21]. The identification of KIT exon mutation was needed for the accurate selection of patients to treat with TKIs in clinical practice. Regarding to the invasive procedure of genotype examination, radiomics as a prospective non-invasive method was extensively applied in tumor diagnosis in recent years [22]. In this study, we developed a CT radiomics-based model for the prediction of GISTs gene mutation. Our results showed that CT texture analysis could potentially be used to differentiate GISTs with KIT 11 exon

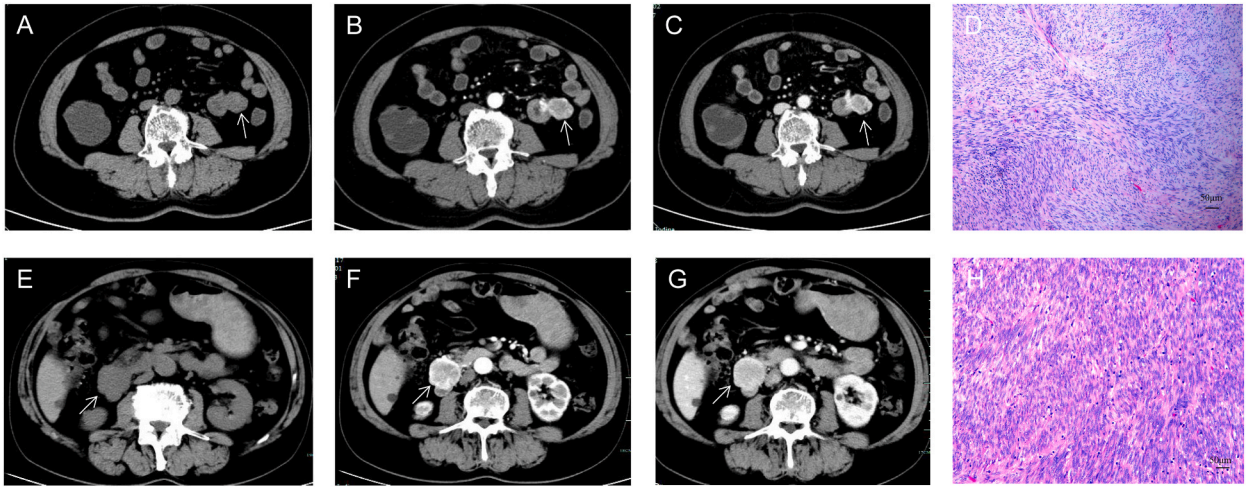


**Fig. 4.** Two GIST patients without (upper) and with (below) KIT Exon 11 mutation. Similar imaging findings were observed on conventional (A, E), arterial (B,F), venous (C, G) and phases. Similar histological features (D, H) were observed in the two cases. There were differences in X453 (0.52 vs 0.43), X629 (4.60 vs 5.10), and X680 (42.71 vs 36.52).

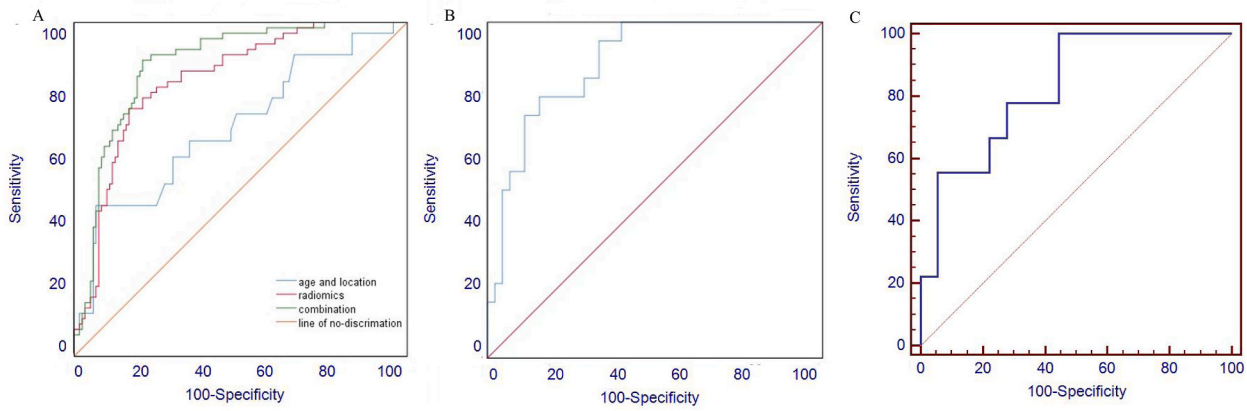


**Fig. 5.** The performance of clinical, radiomics and combined models in identifying KIT 11 mutation in training (A), internal validation group (B) and external validation group (C).

mutation from those without KIT 11 exon mutation.

Hirota et al. [23] first found that proto-oncogene receptor tyrosine kinase KIT mutations occurred in the transmembrane protein and tyrosine kinase regions caused continuous activation of the KIT mutant protein in the GISTs in the absence of ligand. This finding suggests that mutations in the KIT gene dominate the occurrence of the GISTs. Other research groups confirmed these findings at the same time by reporting similar findings and that KIT was a more sensitive and specific marker than CD34 for GISTs [24]. KIT mutations typically affected the juxtamembrane domain encoded by exon 11 [2]. Previous studies showed that KIT exon 11 mutation accounted for a range from 61 % to 93.8 % of KIT mutations and was an independent prognostic factor for progression-free survival and overall survival of GISTs [4,25,26]. In this study, we found 71 % (45 of 63) GIST patients involved KIT exon 11 mutation. GIST patients with KIT exon 11 deletion mutation had lower risk of progression than those with KIT exon 9 mutation and were well responded to longer adjuvant treatment of imatinib [23,27]. Several studies had indicated that GIST patients with KIT exon mutation were benefit from imatinib treatment before surgery [2]. It was recommended that imatinib should be administered for 2–6 months before tumor resection [28]. Most of lesions decreased in size and vascular density after preoperative imatinib treatment which facilitated tumor resection or organ-sparing surgery [29]. For this reason, preoperative KIT exon mutation detection should be done to identify patients who were not respond well to imatinib treatment.

Radiomics is able to extract large amounts of quantitative features from medical images and the quantitative analysis of these features could diminish subjective factors. Previous studies had predicted the malignant potential of GISTs by developing nomograms based on clinical features and radiomics intensity values. Wang et al. [11] developed a nomogram including tumor maximum diameter, tumor location and intensity value range to differentiate high-from low-malignant potential GISTs with an AUC of 0.882. Several studies also developed radiomics-based model to predict the malignant potential of GISTs [10,30,32], the mitotic index and

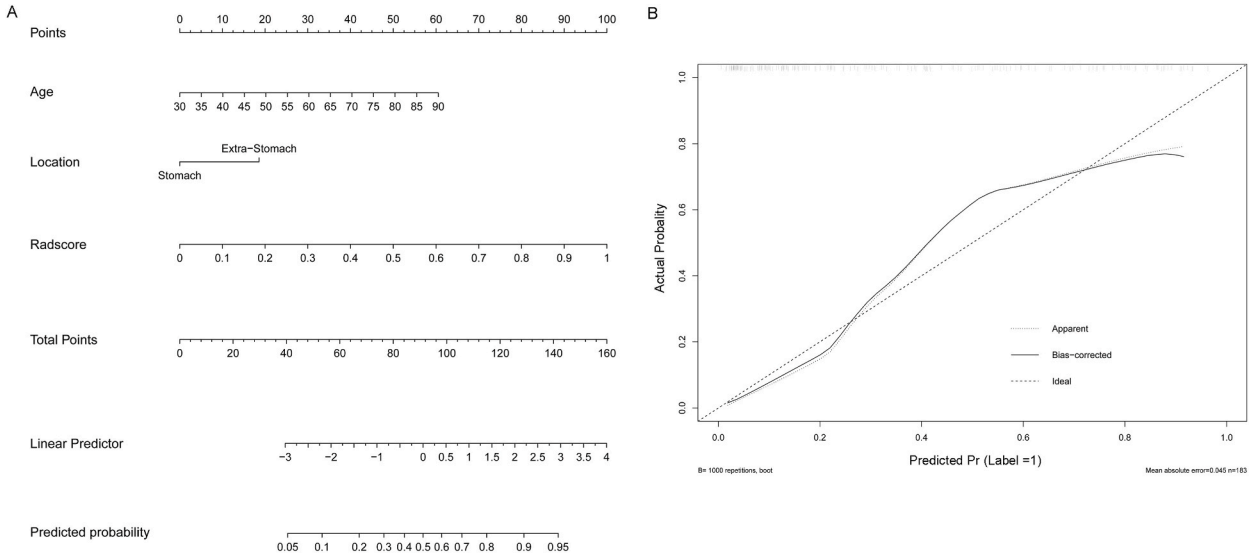


**Fig. 6.** The nomogram for identifying GISTs without KIT 11 mutation (A) and the calibration curve (B). Calibration curve showed good performance.

risk classification of GISTs [31] or prediction of Ki-67 expression in GISTs [33]. GLCM and GLRLM features which indicated the brightness or mean gray-level intensity of a region were the commonly useful radiomics features in those studies. GLCM features might also represent the contrast, complexity and heterogeneity of local intensity patterns. In our study, we also found that X453, a GLCM feature, was an independent predictable factor for KIT exon 11 mutation. To the best of our knowledge, few study haven shown the role of radiomics in GIST gene mutation. A recent study indicated that the combination of conventional CT image analysis and texture analysis was useful to distinguish GISTs with KIT exon 11 mutation [5]. However, that study did not show the independent role of radiomics. Our study showed that both radiomics model and the combined model had good performance in identifying KIT exon 11 mutation. We also developed a nomogram which showed good performance.

In the present study, we amplified the samples using oversampling method to balance the data because the small sample size of GISTs without KIT 11 mutation. Oversampling method has been used in many studies for data balance. Kocak et al. [19] developed a radiomics model for predicting PBRM1 gene subtype of renal clear cell carcinoma by resampling which was the mainstream subclass oversampling and major class undersampling. Feng et al. [34] also conducted a radiomics study to identify BAP1 mutation status in renal clear cell carcinoma using oversampling and resampling methods which decreased overfitting by increasing the randomness of the data. Xu et al. [35] also applied resampling method to the prediction of KIT mutation in GISTs. They used 2D ROI to segment tumors and oversampled tumor data for balance. The study compared 2D ROI with volume ROI, resulting in a good consistency.

Our study had several limitations that should be noted. Firstly, as a single-center retrospective study, there were inherent shortcomings. Secondly, the sample size was small, and the machine learning model had the risk of overfitting. Thirdly, only 2D texture features were used in this study, without 3D texture and morphological features. However, many segmentation studies based on single segmentation or several slices had achieved good results [36,37]. Fourthly, there were limited types of mutations in the exon of the GISTs, whereas the number of cases of mutations in exon 18 of the GISTs and in exon 9 of the KIT GISTs were relatively few and could only be generalized into the group of non-Kit exon 11 GISTs. However, the subtypes of exon 18 and exon 9 might be more valuable and worthy of further study. Fifth, IBEX was used for texture extraction. However, several studies reported that some radiomics features or preprocessing methods in IBEX are not aligned with image biomarker standardization initiative (IBSI) [38,39]. It would be interesting to used software that claim compatibility with the IBSI standard. Finally, potential differences between data in imaging studies and small samples used for genomic analysis might be considered as another potential bias, which was also considered a common problem in most imaging and genetic studies [40].

In summary, we established an objective, non-invasive radiomics model that showed good performance in predicting KIT exon 11 mutation of GISTs. It can be an effective tool to help clinicians accurately predict the mutation of KIT exon 11 in GISTs and provide more personalized precise decision of imatinib therapy.

## Ethics statement

This study was approved by the institutional review board of the First Affiliated Hospital of Zhejiang University School of Medicine (2017NL-137).

## Funding statement

None.

## Data availability statement

The data associated with our study was not deposited into a publicly available repository. Data will be made available on request.

## Additional information

No additional information is available for this paper.

## CRediT authorship contribution statement

**Chuangen Guo:** Conceptualization, Data curation, Formal analysis, Writing – original draft, Writing – review & editing. **Hao Zhou:** Data curation, Formal analysis, Writing – original draft, Writing – review & editing. **Xiao Chen:** Conceptualization, Data curation, Formal analysis, Writing – original draft, Writing – review & editing. **Zhan Feng:** Conceptualization, Data curation, Formal analysis, Writing – review & editing.

## Declaration of competing interest

The authors declare that they have no known competing financial interests or personal relationships that could have appeared to influence the work reported in this paper.

## Acknowledgement

None.

## References

[1] S. Hirota, K. Isozaki, Pathology of gastrointestinal stromal tumors, Pathol. Int. 56 (1) (2006) 1–9.
[2] H. Joensuu, P. Hohenberger, C.L. Corless, Gastrointestinal stromal tumour, Lancet 382 (9896) (2013) 973–983.
[3] S. Bauer, M.C. Heinrich, S. George, J.R. Zalcberg, C. Serrano, H. Gelderblom, et al., Clinical activity of ripretinib in patients with advanced gastrointestinal stromal tumor harboring heterogeneous kit/pdgfra mutations in the Phase III INVICTUS Study, Clin. Cancer Res. 27 (23) (2021) 6333–6342.
[4] T.T. Liu, C.F. Li, K.T. Tan, Y.H. Jan, P.H. Lee, C.H. Huang, et al., Characterization of aberrations in dna damage repair pathways in gastrointestinal stromal tumors: the clinicopathologic relevance of γH2AX and 53BP1 in correlation with heterozygous deletions of CHEK2, BRCA2, and RB1, Cancers 14 (7) (2022) 1787.
[5] J. Andersson, P. Bumming, J.M. Meis-Kindblom, H. Sihto, N. Nupponen, H. Joensuu, et al., Gastrointestinal stromal tumors with KIT exon 11 deletions are associated with poor prognosis, Gastroenterology 130 (6) (2006) 1573–1581.
[6] R. Quek, M. Farid, Y. Kanjanapan, C. Lim, I.B. Tan, S. Kesavan, et al., Prognostic significance of KIT exon 11 deletion mutation in intermediate-risk gastrointestinal stromal tumor, Asia Pac. J. Clin. Oncol. 13 (3) (2017) 115–124.
[7] X. Liu, Y. Yin, X. Wang, C. Yang, S. Wan, Y. Yin, et al., Gastrointestinal stromal tumors: associations between contrast-enhanced CT images and KIT exon 11 gene mutation, Ann. Transl. Med. 9 (19) (2021) 1496.
[8] D. Scola, L. Bahoura, A. Copelan, A. Shirkhoda, F. Sokhandon, Getting the GIST: a pictorial review of the various patterns of presentation of gastrointestinal stromal tumors on imaging, Abdom. Radiol (NY) 42 (5) (2017) 1350–1364.
[9] F. Vernuccio, R. Cannella, A. Comelli, G. Salvaggio, R. Lagalla, M. Midiri, Radiomics and artificial intelligence: new frontiers in medicine, Recenti Prog. Med. 111 (3) (2020) 130–135.
[10] J. R, P.E. Kinahan, H. Hricak, Radiomics: images are more than pictures, They Are Data, Radiology. 278 (2) (2016) 563–577.
[11] P. Lambin, E. Rios-Velazquez, R. Leijenaar, S. Carvalho, R.G. van Stiphout, P. Granton, et al., Radiomics: extracting more information from medical images using advanced feature analysis, Eur. J. Cancer 48 (4) (2012) 441–446.
[12] T. Chen, Z. Ning, L. Xu, X. Feng, S. Han, H.R. Roth, et al., Radiomics nomogram for predicting the malignant potential of gastrointestinal stromal tumours preoperatively, Eur. Radiol. 29 (3) (2019) 1074–1082.
[13] C. Wang, H. Li, Y. Jiaerken, P. Huang, L. Sun, F. Dong, et al., Building CT radiomics-based models for preoperatively predicting malignant potential and mitotic count of gastrointestinal stromal tumors, Transl. Oncol. 12 (9) (2019) 1229–1236.
[14] E. Ozkan, A. West, J.A. Dedelow, B.F. Chu, W. Zhao, V.O. Yildiz, et al., CT gray-level texture analysis as a quantitative imaging biomarker of epidermal growth factor receptor mutation status in adenocarcinoma of the lung, AJR Am. J. Roentgenol. 205 (5) (2015) 1016–1025.
[15] C.A. Karlo, P.L. Di Paolo, J. Chaim, A.A. Hakimi, I. Ostrovnaya, P. Russo, et al., Radiogenomics of clear cell renal cell carcinoma: associations between CT imaging features and mutations, Radiology 270 (2) (2014) 464–471.
[16] L.J. Grimm, J. Zhang, M.A. Mazurowski, Computational approach to radiogenomics of breast cancer: luminal A and luminal B molecular subtypes are associated with imaging features on routine breast MRI extracted using computer vision algorithms, J. Magn. Reson. Imag. 42 (4) (2015) 902–907.
[17] F. Giganti, P. Marra, A. Ambrosi, A. Salerno, S. Antunes, D. Chiari, et al., Pre-treatment MDCT-based texture analysis for therapy response prediction in gastric cancer: comparison with tumour regression grade at final histology, Eur. J. Radiol. 90 (2017) 129–137.
[18] N.V. Chawla, K.W. Bowyer, L.O. Hall, W.P. Kegelmeyer, SMOTE: synthetic minority over-sampling technique, J. Artif. Intell. Res. 16 (2002) 321–357.
[19] B. Kocak, E.S. Durmaz, E. Ates, M.B. Ulusan, Radiogenomics in clear cell renal cell carcinoma: machine learning-based high-dimensional quantitative ct texture analysis in predicting pbrm1 mutation status, AJR Am. J. Roentgenol. 212 (3) (2019) W55–W63.
[20] J. Du, S. Wang, R. Wang, S. Wang, Q. Han, H.T. Xu, et al., Identifying secondary mutations in Chinese patients with imatinib-resistant gastrointestinal stromal tumors (GISTs) by next generation sequencing (NGS), Pathol. Oncol. Res. 26 (1) (2020) 91–100.
[21] H. Joensuu, E. Wardelmann, H. Sihto, M. Eriksson, K. Sundby Hall, et al., Effect of kit and pdgfra mutations on survival in patients with gastrointestinal stromal tumors treated with adjuvant imatinib: an exploratory analysis of a randomized clinical Trial, JAMA Oncol. 3 (5) (2017) 602–609.

[22] M. Wang, Z. Feng, L. Zhou, L. Zhang, X. Hao, J. Zhai, Computed-Tomography-Based Radiomics Model for predicting the malignant potential of gastrointestinal stromal tumors preoperatively: a multi-classifier and multicenter study, Front. Oncol. 11 (2021), 582847.
[23] S. Hirota, K. Isozaki, Y. Moriyama, K. Hashimoto, T. Nishida, S. Ishiguro, et al., Gain-of-function mutations of c-kit in human gastrointestinal stromal tumors, Science 279 (5350) (1998) 577–580.
[24] M. Sarlomo-Rikala, A.J. Kovatich, A. Barusevicius, M. Miettinen, CD117: a sensitive marker for gastrointestinal stromal tumors that is more specific than CD34, Mod. Pathol. 11 (8) (1998) 728–734.
[25] G. Palomba, P. Paliogiannis, M.C. Sini, M. Colombino, M. Casula, A. Manca, et al., KIT and PDGFRa mutational patterns in Sardinian patients with gastrointestinal stromal tumors, Eur. J. Cancer Prev. 30 (1) (2021) 53–58.
[26] Z. Szucs, K. Thway, C. Fisher, R. Bulusu, A. Constantinidou, C. Benson, et al., Molecular subtypes of gastrointestinal stromal tumors and their prognostic and therapeutic implications, Future Oncol. 13 (1) (2017) 93–107.
[27] A. Patrikidou, J. Domont, S. Chabaud, et al., Long-term outcome of molecular subgroups of GIST patients treated with standard-dose imatinib in the BFR14 trial of the French Sarcoma Group, Eur. J. Cancer 52 (2016) 173–180.
[28] D. Wang, Q. Zhang, C.D. Blanke, G.D. Demetri, M.C. Heinrich, J.C. Watson, et al., Phase II trial of neoadjuvant/adjuvant imatinib mesylate for advanced primary and metastatic/recurrent operable gastrointestinal stromal tumors: long-term follow-up results of Radiation Therapy Oncology Group 0132, Ann. Surg Oncol. 19 (4) (2012) 1074–1080.
[29] B.L. Eisenberg, J.C. Trent, Adjuvant and neoadjuvant imatinib therapy: current role in the management of gastrointestinal stromal tumors, Int. J. Cancer 129 (11) (2011) 2533–2542.
[30] C. Ren, S. Wang, S. Zhang, Development and validation of a nomogram based on CT images and 3D texture analysis for preoperative prediction of the malignant potential in gastrointestinal stromal tumors, Cancer Imag. 20 (1) (2020) 5.
[31] L. Yang, T. Zheng, Y. Dong, Z. Wang, D. Liu, J. Du, et al., MRI texture-based models for predicting mitotic index and risk classification of gastrointestinal stromal tumors, J. Magn. Reson. Imag. 53 (4) (2021) 1054–1065.
[32] Y. Song, J. Li, H. Wang, B. Liu, C. Yuan, H. Liu, et al., Radiomics nomogram based on contrast-enhanced ct to predict the malignant potential of gastrointestinal stromal tumor: a two-center study, Acad. Radiol. 29 (6) (2022) 806–816.
[33] Q.W. Zhang, Y.J. Gao, R.Y. Zhang, X.X. Zhou, S.L. Chen, Y. Zhang, et al., Personalized CT-based radiomics nomogram preoperative predicting Ki-67 expression in gastrointestinal stromal tumors: a multicenter development and validation cohort, Clin. Transl. Med. 9 (1) (2020) 12.
[34] Z. Feng, L. Zhang, Z. Qi, Q. Shen, Z. Hu, F. Chen, Identifying bap1 mutations in clear-cell renal cell carcinoma by ct radiomics: preliminary findings, Front. Oncol. 10 (2020) (2020) 279.
[35] F. Xu, X. Ma, Y. Wang, Y. Tian, W. Tang, M. Wang, et al., CT texture analysis can be a potential tool to differentiate gastrointestinal stromal tumors without KIT exon 11 mutation, Eur. J. Radiol. 107 (2018) 90–97.
[36] M.R.M. Sun, N. Long, E.M. Genega, M.B. Atkins, M.E. Finn, N.M. Rofsky, et al., Renal cell carcinoma: dynamic contrast-enhanced MR imaging for differentiation of tumor subtypes–correlation with pathologic findings, Radiology 250 (3) (2009) 793–802.
[37] Z. Feng, Q. Shen, Y. Li, Z. Hu, CT texture analysis: a potential tool for predicting the Fuhrman grade of clear-cell renal carcinoma, Cancer Imag. 19 (1) (2019) 6.
[38] I. Fornacon-Wood, H. Mistry, C.J. Ackermann, et al., Reliability and prognostic value of radiomic features are highly dependenton choice of feature extraction platform, Eur. Radiol. 30 (11) (2020) 6241–6250.
[39] A. Bettinelli, M. Branchini, F. De Monte, A. Scaggion, M. Paiusco, Technical Note: an IBEX adaption toward image biomarker standardization, Med .Phys. 47 (3) (2020) 1167–1173.
[40] F. Alessandrino, A.B. Shinagare, D. Bossé, T.K. Choueiri, K.M. Krajewski, Radiogenomics in renal cell carcinoma, Abdom. Radiol. (NY) 44 (6) (2019) 1990–1998.